UCRL-10071

University of California

Ernest O. Lawrence Radiation Laboratory

Berkeley, California

DISCLAIMER

UCLA Conference on Sector-Focused Cyclotrons
April 17-20, 1962

UCRL-10071

UNIVERSITY OF CALIFORNIA

Lawrence Radiation Laboratory
Berkeley, California

Contract No. W-7405-eng-48

CENTER-REGION GEOMETRY OF THE BERKELEY 88-INCH CYCLOTRON

Hans A. Willax and Alper A. Garren

April 16, 1962

CENTER-REGION GEOMETRY OF THE BERKELEY 88-INCH CYCLOTRON

Hans A. Willax and Alper A. Garren

Lawrence Radiation Laboratory
University of California
Berkeley, California

April 16, 1962

ABSTRACT

In order to determine the proper position of the dee edge, ion source, puller, and beam-defining clipper with respect to the magnet center, measurements of the structure of the electric field in the surroundings of the ion source were made with a half-scale model in an electrolytic tank. The acceleration process during the first three revolutions was studied for different geometries and starting phases, by a graphical approximation method for orbit plotting. A more detailed study was then made to determine initial conditions—such as orbit-center distribution, energy spread, axial focusing, and energy bunching—as functions of the center geometry and starting phase. By increasing the particle path length during the first half revolution approximately 20 deg—achieved by azimuthal displacement of the source—good results were obtained. The ion-start location was finally determined so as to bring the beam close to an equilibrium orbit at 10 in. radius. This was done with an orbit code, modified to take account of the increased transit time through the acceleration gap of smaller radii. Some experimental results of changes in the cyclotron beam quality, caused by changes in the ion-starting conditions, are presented.

CENTER-REGION GEOMETRY OF THE BERKELEY 88-INCH CYCLOTRON†

Hans A. Willax†† and Alper A. Garren

Lawrence Radiation Laboratory
University of California
Berkeley, California

April 26, 1962

1. Introduction

For efficient extraction of the beam from an isochronous cyclotron, a good quality of the internal beam is required at the extraction radius[1-4]). Any practical beam-extraction device based on the electrostatic, magnetic, or regenerative principle effectively accepts only a rather limited area of the radial and axial phase space. A high relative particle density in this phase space range is desirable. Among the parameters that affect the particle distribution in the axial and radial phase space during the whole acceleration process, we are to consider those which counteract the beam-focusing forces, such as space-charge effects or perturbations in the magnetic field. A closer consideration of the starting conditions of the ions, and a quantative evaluation of the effects of the electric field on the low-energy particles near the ion source, seems especially important. It is believed that the radial and axial phase space proper for extraction from the machine can already be defined to a certain extent at the machine center, and can be filled with a relatively large number of particles by an appropriate choice of the starting conditions.

Many experimenters[2]) observed phenomena on cyclotron beams that are related to the starting conditions or the influence of the electric field in the

---

† Work done under the auspices of the U. S. Atomic Energy Commission.

†† Permanent address: Swiss Federal Institute of Technology, Zurich.

center of a cyclotron. Theoretical investigations of focusing effects and phase-bunching effects were made by Cohen[5]), Tinta[6]), Konrad[7]), Reiser[8]), and others under somewhat idealized assumptions of the electric-field configuration near the ion source. These assumptions allowed a clear mathematical treatment, and are justified for symmetrical geometries with two dees or dee and dummy-dee configurations.

The 88-inch cyclotron was designed for a single dee, and, if possible, we wanted to eliminate a dummy dee in order to provide more flexibility for the ion-source position, and easy access to the machine center for probes, etc. We made a study of the electric field configuration in the acceleration gap for a single-dee geometry and for a dee and dummy-dee configuration. The study was based on an analog method with conductivity paper[9]), and investigations about the electric field geometry around the ion source on a half-scale model in an electrolytic tank. Phase and orbit-center bunching effects were evaluated for the first three particle revolutions by using a geometrical orbit-approximation method[10]). The proper range of starting phases could be estimated from numerical evaluation of the electric focusing forces during the first six gap crossings.

We found that in our case a dummy dee is not needed if the ion source can be used in combination with a puller electrode protruding from the dee. The lack of a dummy dee even increases the axial focusing properties, besides offering full flexibility for positioning of the ion source with respect to the magnet center for different magnetic field levels and different charge-to-mass ratios of the particles.

In order to increase the electric axial focusing during the initial few revolutions in a region where no magnetic focusing could be expected, the path length during the first half revolution was increased by approximately

20 deg, in accordance with a proposal by Smith[11]). The phase lag could be compensated by a magnetic field cone, [12]) which also carried the magnetic focusing out to a radius of approximately 6 in., where the field flutter becomes effective.

In order to estimate the phase-acceptance range of an axially and radially well-behaved beam, as well as the source-output efficiency, the initial acceleration process between ion-source opening and puller electrode was studied more carefully. From these studies the proper configuration of the puller electrode, its position, and the position of the ion source could be derived. A final correction was made in order to make the most favorable starting orbit coincide with an equilibrium orbit at 10 in. magnet radius. This correction entailed deceleration computations from 10 in. inwards which used the actual magnetic field and an empirically derived transit-time factor for the energy gain at smaller radii.

A series of measurements of the radial and axial beam behavior for different starting geometries was made with α particles at 11.7 kG during preliminary operation of the 88-inch cyclotron. The results show that the cyclotron beam quality can be largely affected by the ion-source puller geometry. The effects observed are in general in agreement with theoretical predictions, and confirm the assumptions made for the evaluation of the beam starting conditions.

2. Measurements of the Electric Field in the Vicinity of the Ion Source

The shape of the electric field across the dee gap was measured in an undisturbed region by applying the analog method with conductivity paper[9]). Figure 1a shows the equipotential lines in a vertical cross section across the dee gap for a single dee, and fig. 1b for a dee and dummy-dee configuration. In fig. 2a comparison is made of the fall-off of the electric potential in both

cases. Figure 2b shows the horizontal components of the electric field strength in the median plane, and fig. 2c the vertical components at a distance of 1/4 in. from the median plane. The numerical quantities are based on maximum dee voltage of 70 kV. The relationships shown are valid beyond a distance of about 5 in. from a field-perturbing object, such as the ion source or the puller. The asymmetry with respect to the center of the acceleration gap is obvious; however it is not so distinct when a dummy dee is present.

To investigate the configuration of the electric field around the source, a three-dimensional half-scale model of the physical structure in the center region was used for measurements in an electrolytic tank. The equipotential lines were measured in a conventional way at the surface of the electrolyte; this surface represented the median plane. The positions of source and puller were approximated from earlier preliminary investigations[10]). Results are shown in figs. 3d and b. The results for a proposed single-dee and a dee and dummy-dee configuration are shown in figs. 3b and c. The perturbation of the electric field, caused by the ion-source being at ground potential, and by the protrusion of the puller beyond the dee, is asymmetrical in these cases. In order to show the relationship between extension of the perturbation and the expected beam path, the first half revolution of deuterons at 16.5 kG, extracted with a voltage of 70 kV, is indicated approximately in the graphs. It can be demonstrated that, with the configurations present, the assumption of uniform fields across the acceleration gap is certainly not justified for the first few beam revolutions. The particles spend a large fraction of the rf cycle in an electric field of varying directions. The time-of-flight effect differs markedly at each gap. Especially in the case of a single puller rod, as shown in fig. 4, a rather strong effect of phase bunching, accompanied by distortion of the radial beam quality, can be expected[10]). (This effect is a result of the strong orbit orthogonal forces of the electric field on the low-energy ions).

Since good radial beam quality was more desirable than a strong phase-bunching effect, the puller configuration of fig. 3 seemed satisfactory; all further investigations were concentrated on such a geometry. In this configuration the influence of the electric field ceases rather abruptly once the particles have passed the puller slit. By the time the particles have passed through the low-electric-field region which follows the slit, the *rf* phase has changed. Nevertheless, the transit-time effect, resulting in a relative decrease of energy gain per gap cross, has to be taken into account for the first few revolutions.

3. Particle Acceleration on the First Turns

First investigations of the acceleration process affecting the innermost revolutions were made for particles with a charge-to-mass ratio of 1/2, with the aid of a geometric orbit-approximation method [10]. We used a radially constant magnetic field of 16.5 kG and the accelerating electric field as measured in the electrolytic tank under the assumption of 70-kV dee voltage. In this analog method of orbit construction, the acceleration of ions in the extended electric field was simulated by a step-by-step momentum gain for each 30 deg of the rf cycle, where the rf frequency was taken to be equal to the cyclotron frequency $\omega_0 = \frac{qe}{Am} \times H$. A rather accurate evaluation of particle location, particle energy, and apparent center of motion as a function of time was possible. By applying this method to ions with different starting phases—such as 30 deg leading, in phase, or 30 deg lagging—it was possible to estimate the behavior of an expected beam pulse, its phase bunching, and its energy or center bunching.

The results over the first three revolutions for a single dee and a dee and dummy-dee configuration are shown in fig. 5. The anticipated radial width of a beam pulse consisting of particles with starting phases from +30 deg (leading) to -30 deg (lagging) is shaded in this figure. Noticeable in fig. 5 are the large

radial extent of the beam pulse after 1/2 + n revolutions and its radial concentration on the rear side of the ion source, as well as overlapping beam regions. Also indicated are the beam pulse shape and the apparent orbit centers of the particles after the third revolution.

For a quantitative evaluation of the two dee configurations, one can compare the energy spread, the center spread, and the phase spread of the pulse after the ion have left the region of the electric-field perturbation near the ion source. In our case this is approximately after the third revolution. The values obtained for the two configuration are listed in table 1.

Table 1

Beam pulse parameters after third revolution

	Starting phase	Single dee	Dee+dummy dee
Energy	+30 deg(leading)	395 keV	409 keV
	0 deg(in phase)	361 keV	393 keV
	-30 deg(lagging)	256 keV	301 keV
Average energy		338 keV	368 keV
Energy spread		139 keV	368 keV
Center spread		0.2 in.	0.3 in.
Phase contraction (60 deg initial pulse width)		≈ 5 deg	≈ 10 deg

With regard to particle motion close to the median plane, it does not seem necessary to provide a dummy dee in this case. As a comparison of the listed beam pulse parameters shows, the relative decrease of the energy spread obtainable with a dummy dee is small. There is even indication of a somewhat larger spread of orbit centers with a dummy dee present. The relative phase concentration is small in both geometries.

Evaluation of the electric axial focusing properties leads here to results in favor of a single-dee geometry. This can be explained by the fact that in the single-dee geometry the electric axial focusing is larger after 1/2 + n revolutions because of the asymmetry in the vertical component of the electric field. After each full revolution the particles pass through a very similar axial field configuration in both cases. This configuration is largely affected by the vertical shape of the ion source and puller.

Note that the essential energy gain per gap cross is diminished by the time-of-flight effect. For numerical orbit computations with a digital computer, where one wants to idealize the acceleration process by a step momentum gain at the center of the dee gap, a transit-time factor f(R) for the energy gain per gap cross has been derived from the graphical orbit studies. With this idealization the energy gain during the first few gap crossings can be expressed by $\Delta e = q \cdot f(R)\, U_0 \cos(\omega t - \phi)$, for particles in a phase range from +30 deg to -30 deg. The transit-time factor is shown in fig. 6 as a function of radius. The asymmetry for the gap crossings south and north is obvious.

In order to obtain information about the influence of the perturbed electric field on the radial beam behavior during the first few revolutions, an orbit study was made for two particles with a starting angular divergence corresponding to ± 1/8 in. radial amplitude, as shown in fig. 7. No severe distortion could be noticed.

For closer investigation of the electric axial focusing near the center, the dee gaps were considered as electrical lenses that change their optical coefficient of refraction according to the time variation of the electric field. Particle trajectories with an original vertical displacement of ±0.25 in. were computed numerically for starting phases of +30, 0, and -30 deg. From the angular deviation at each gap crossing, the equivalent axial betatron frequency $\nu_{z\,el}$ could be evaluated. Figure 8 shows the values of $\nu_{z\,el}^2$ for the first

three revolutions, as derived in this manner. Since the electric axial focusing drops rather fast with increasing radius, the magnetic axial focusing has to be brought close to the center. In the 88-inch cyclotron the magnetic field flutter becomes effective at radii larger than 6 in.; therefore, it seemed feasible to provide axial focusing in the transition region by a radially falling field. Essentially, it was believed that the axial focusing in the region out to 6 in. should be high because of possible space-charge effects at higher beam intensities. Therefore, a rather steep center cone of the magnetic field was proposed[12]). This cone could simultaneously compensate for a phase lag on the order of 10 to 20 deg—necessary for strong electric axial focusing at the first 3 revolutions. In fig. 8 we also show the magnetic axial focusing term resulting from this field cone. In this manner a good transition in axial focusing can be obtained for particles with phases smaller than ±5 deg at the first half revolution; the optimal conditions are obtainable for ions with a phase lag of ≈ 20 deg at the first revolution.

4. Computation of the Proper Ion-Source Location

For proper location of the ion source and the ion puller we try to meet these requirements:

a. The source has to be placed so that it ejects particles with a high output efficiency into a rf phase range, where axial electric focusing takes place at the first three revolutions.

b. The energy spread of the beam pulse accepted by the cyclotron should be small compared to the initial energy gain.

c. The spread of orbit centers for particles of the accepted pulse should not be larger than the optimal radial beam amplitude, in this case ± 1/8 in.

d. The apparent orbit center of the beam pulse should coincide with the magnet center, once the beam reaches a symetrical electric field configuration and a symmetrical magnetic field.

Since the machine is also designed to accelerate heavy ions to different energies, all these requirements have to be met for different e/m, different magnetic field levels, and different acceleration voltages.

For a prediction of the ion source and puller location we used an x-y coordinate system with the origin at the source slit, as indicated in fig. 9. The x-y system is rotated with respect to the cyclotron coordinate system x'-y' by an angle γ, and has a certain displacement from the magnet center which should be defined by the magnitudes a, b, and Y, the initial displacement of the orbit center (fig. 9). From the equations of particle motion in the median plane in the x-y coordinate system

$$\left.\begin{aligned} \ddot{x} &= \frac{e}{m}\left\{E_x(x, y)\cos(\omega t-\phi) + \dot{y}\,B(x, y)\right\}, \\ \ddot{y} &= \frac{e}{m}\left\{E_y(x, y)\cos(\omega t-\phi) - \dot{x}\,B(x, y)\right\}. \end{aligned}\right\} \qquad (1)$$

for the initial acceleration one can derive eqs. (2), (3), and (4), assuming:

a. The rf frequency corresponds to the cyclotron frequency at the center field.

b. The particles, being accelerated from zero velocity at x, y = 0, pass through a uniform electric field which has no y component, and which ceases at the puller slit.

c. The magnetic field is uniform in the range of the first half revolution.

d. Space charge effect can be neglected for the motion in the median plane.

$$x(t, \phi_0) = \frac{e\,E_0}{2m\omega^2}\overbrace{[\sin\phi_0 \sin\omega t + \omega t \sin(\omega t-\phi_0)]}^{\chi(\omega t, \phi_0)}, \qquad (2)$$

$$Y(t,\phi_0) = \frac{e E_0}{m\omega^2}\overbrace{[\sin\phi_0 + \sin(\omega t-\phi_0)]}^{\eta(\omega t,\phi_0)}, \qquad (3)$$

$$\epsilon(t,\phi_0) = \frac{e^2E^2_0}{8m\omega^2}\left\{\overbrace{[\sin\phi_0\cos\omega t+\sin(\omega t-\phi_0)+\omega t\cos(\omega t-\phi_0)]^2}^{\Lambda(\omega t,\phi_0)} + [\sin\phi_0\sin\omega t+\omega t\sin(\omega t-\phi_0)]^2\right\}, \qquad (4)$$

where

E_0 = maximum electric field strength,

ϕ_0 = starting phase ($\phi_0 > 0$ = leading, $\phi_0 < 0$ = lagging).

Considering the accuracy with which one wants to determine the location of a particle x, its initial displacement of the center of motion Y, and its initial energy ϵ at the puller slit, these assumptions seem to be justified.

Under the assumption of a uniform electric field, $E = U_0/d\cos(\omega t-\phi_0)$, which points into the x direction only, the apparent center of particle motion during the acceleration process between source slit and puller slit remains on the y axis (fig. 9). It freezes at Y, once the particle passes through the puller slit into a field-free region at point P. At this point the ion has the energy ϵ and describes an arc around Y, with the radius R, which corresponds to the particle momentum and the magnetic field present, until the particle again reaches a region of acceleration. Equations (5), (6), and (7) show the relationship for d, Y, and ϵ in practical units.

$$d = \frac{2.285}{B_{ie}}\sqrt{\frac{A}{q}}\sqrt{U_0}\sqrt{\chi(\tau,\phi_0)} \quad \text{(cm)} \qquad (5)$$

$$Y = \frac{4.57}{B_{is}} \sqrt{\frac{A}{q}} \sqrt{U_0} \sqrt{\frac{\eta(\tau, \phi_0)}{\chi(\tau\phi_0)}} \quad \text{(cm)}, \qquad (6)$$

$$\epsilon = \frac{1.275 U^2_0}{B_{is}{}^2 \cdot d^2} \cdot A \left\{ \Lambda(\tau, \phi_0)^2 + \chi(\tau, \phi_0)^2 \right\} \quad \text{(keV)}, \qquad (7)$$

where

B_{is} = isochronous magnetic field of the machine center, in kilogauss,

U_0 = maximum dee voltage, in kilovolts,

A = atomic weight of particle,

q = number of charge units,

τ = transit-time angle.

For a given puller distance d, both the initial energy and the initial orbit center for an ion at P are functions of the applied voltage U_0, the charge-to-mass ratio q/A, the starting phase ϕ_0, and the transpired phase change (ωt_p), which shall be called transit phase angle τ. For a given q/A at a certain magnetic field and an existing geometry and voltage, Y and ϵ are functions of the starting phase ϕ_0 only, as long as space-charge effects remain small. Figure 10 shows the expected initial energy gain ϵ and the initial orbit center coordinate Y as functions of the starting phase ϕ_0, and also as functions of the phase at the puller slit ϕ_p, for two cases of a distinct ion-source to puller distance--corresponding to a transit phase angle of ≈20 and ≈60 deg. The relationships were computed for α particles in a magnetic field of 11.7 kG. The dee-voltage U_0 was 36 kV; ϵ and Y are plotted relative to the maximal values ϵ_m = 72 keV and Y_m = 3.13 cm.

Note that in fig. 10a and c both the ϵ and Y curves are asymmetrical with respect to the zero starting phase. Late-starting particles obviously experience a larger spread in initial energy gain and in their center distribution

than particles starting before the electric field reaches its maximum.

An acceptable beam pulse in our case should not have a relative center spread or energy spread in excess of 10 to 15% Therefore one has to select a group of particles starting from the source at leading phase, as indicated in fig. 10 by the sections A and B. The range of starting phases for a useful beam pulse shifts more towards the leading side as the distance between the source and puller becomes larger, i.e., as the transit time becomes larger. This also means that the axial electric focusing between ion source and puller becomes worse with increasing distance.

Furthermore, since the source extraction efficiency depends on the extracting field approximately to the 3/2 power[13]), beam intensity decreases rapidly with increasing distance between the source and the puller. The ratio of the expected beam intensities for our two examples are indicated by the shaded areas A and B in fig. 10e. It seems very desirable to bring the puller as close to the source as sparking limitations will permit. For axial focusing between source and puller it is necessary to provide adequate vertical components of the electric field close to the source slit, where the particles spend a large fraction of the transit time. We believed that a combination of space-charge effects of the moving plasma boundaries could be important for the axial focusing at the initial acceleration. However, at the time of our design studies these effects were not explored sufficiently to make well-based assumptions for a theoretical treatment; if difficulties, related to these phenomena, arise at high intensities, it is possible to experimentally develop a satisfying vertical ion-source and puller geometry under actual extraction conditions.

In order to pass the selected beam pulse into the most favorable phase range in the cyclotron, for example, 20 deg lagging after the first half revolution, one has to bring the ion source and puller arrangement farther away from the

dee-even, if necessary, beyond the center of the acceleration gap, as indicated in fig. 10. There is a limit, however, since the whole configuration of the electric field around the source changes with this geometry and could become too asymmetric. This would prevent the apparent center of particle motion from moving towards the magnet center during the next few revolutions. The electric field perturbation, created by the source and puller configuration, together with the configuration of the magnetic field near the cone defines, in a final manner, the displacement and rotation of the x, y coordinate system with respect to the cyclotron coordinate system x'-y'. Thus the magnitudes a and b, and the rotation angle γ, in fig. 9 are defined by the acceleration farther on, whereas d, Y, and θ_s are given by the initial acceleration between source and puller, and the phase requirements for a radially and axially well-focused beam pulse.

We have tried to strike a balance in this quite-delicate interrelationship of physical magnitudes. The source-to-puller distance in the 88-inch cyclotron corresponds to a transit-time phase angle of about 30 deg. The center of the well-accepted beam pulse should have a phase lag of 20 deg at the line of symmetry. This means that the puller face had to come out of the dee lip even beyond the line of symmetry, whereas the face of the source had to be removed from the puller face by ≈ 0.3 in. In a first approximation the orbit behavior near the source was calculated with the geometric approximation methods mentioned above, taking into account the actual electric and magnetic field shape out to ≈ 3 in. radius. For this calculation the rotation of the source was such as to bring the initial orbit center onto the line of symmetry. The requirement of starting the orbits in such a way that they would match an equilibrium orbit at 10 in. radius necessitated more computer calculations. In this calculation, particles were decelerated from 10 in. radius using a modified orbit code.

The real magnetic field shape and the electric transit-time effect, as formerly derived and as shown in fig. 7 were taken into account. The goal of these investigations was to meet the line of symmetry at point P of the puller slit with the correct energy and the correct phase lag. It was achieved after a small number of iterations of starting parameters for the computations. A slight correction in the rotation of the x-y coordinate system towards smaller γ was necessary. For α particles at 11.7 kG and 36-kV dee voltage, the following magnitudes are valid: Y = 1.25 in., a = 0.28 in., b = 0.2 in., γ = 11 deg, θ_s = 25 deg.

In one case the ions have to pass the ν_r = 3/3 resonance at about 5 in. radius[14]). However, as computer calculations show, the radial beam distortion is not severe as long as the initial amplitude of the betatron oscillation remains on the order of ± 1/4 in.

5. Center Geometry

Figure 11 shows the locations of the components in the cyclotron center, arranged for operation with α particles at a central isochronous field of 11.67 kG and 36-kV dee voltage. This arrangement also corresponds to deuterons at a central isochronous field of 16.5 kG and 70-kV dee voltage. Figure 11 indicates the first five revolutions of a particle centered in the beam pulse as derived from computer calculations and geometric orbit plotting (dots) under the assumption of a realistic magnetic field. The end position of the probes is shown.

5.1 ION SOURCE AND PULLER

The whole center geometry, consisting of ion source, puller and defining slit, is adjustable for different charge-to-mass ratios of the ions, different magnetic field levels, and different acceleration voltages. For this purpose the ion source can be placed anywhere within the space as marked by the four end positions (dashed circles)[15, 16]). The source can be rotated 360 deg about its vertical axis. The puller is easily exchangeable and can be moved over the

whole range of the possible ion-source locations. The ion-source face has a cutback, as indicated in fig. 11, for achievement of rather good axial focusing at the initial acceleration between source and puller. The vertical height of the puller slit is large enough to provide a slight asymmetry effect on the vertical component of the electric field. Thus the particles should experience more focusing force during the first third of path length between source and puller than defocusing force during the last part of initial acceleration.

Figure 12 shows a photograph of the present puller device. It consists of a solid carbon piece, which has good rf contact with the dee. In order to provide a more uniform electric field in the gap a 1/8-in. tantalum rod is mounted at the side, where low-energy ions would tend to strike.

For the ion source and puller, special care was taken to provide symmetry with respect to the midplane. Even slight asymmetry of the electric field in the vertical direction, especially during the initial acceleration and the first gap crossing certainly had to be avoided.

5.2 BEAM-DEFINING SYSTEM

In general one cannot avoid having particles with an improper starting phase, and therefore a rather large radial and axial betatron amplitude, accepted by the cyclotron. They are accelerated to a certain energy where they either are lost by defocusing effects or are shifted into a decelerating phase.

In order to keep the beam clean from the beginning, an adjustable beam-defining device will be used at a location within the dee where no further perturbation of the electric field would be caused (fig. 11). This device will permit clipping of particles with wrong phases or large radial betatron amplitudes, without interfering with the well-behaved beam. The defining slit consists of two water-cooled tantalum rods which can be moved radially either simultaneously or with respect to each other. Thus any beam orbit from the

first resolution on outward can be affected, either by passing through the proper slit, or by being scraped on the outside and inside.

6. Experimental Results

During the first period of preliminary operations with α particles at 11.7 kG[17]), it was possible to check the influence of changes in the starting conditions on the beam quality. The defining slit was not yet usable.

The three probes, equally spaced in azimuth (see fig. 11), could each be arranged to pick up current on three separate electrodes. These electrodes have a radial extension of 1-1/2 in. and a vertical height of 1/2 in. each, and are mounted above one another. The probes could also be used to measure beam current on a radial increment of 1/16 in. while the rest of the pickup electrodes in the radial direction were covered by a shield. Thus it was possible to determine the beam centering, as well as the radial and axial beam amplitudes, as functions of the radius.

The ion source and puller were set at theoretically predetermined positions, then the radial beam current distribution was measured at different dee voltages from 2 in. on out. With the radial differential probes it was possible to resolve up to 50 separate revolutions. These revolutions changed their spacing according to changes in the dee voltage. Figure 13 is a perspective view of the center region out to 12 in. radius; current distributions as measured on the dee area probe and the target area probe, are shown here as reliefs. The pickup elements in this case were of 1/16-in. radial width and 1/2-in. axial extent, centered in the median plane. The acceleration voltage was set at a dee-voltage meter reading of 36 kV. The meter had been calibrated at lower voltages.)

The turn-to-turn separation is distinct out to 12 in. radius; 44 separate revolutions can be noticed in this case. The average turn spacing is somewhat

larger than anticipated, indicating that the dee voltage might actually be about 10% higher than the reading on the meter.

The apparent center of motion for the first 15 revolutions was found to be within ±0.1 in. from the predicted locations. The phase acceptance of the beam pulse corresponds approximately to the anticipated value of 30 deg, as the beam width at the first few revolutions indicates.

At about 5 in. radius, close to the $\nu_r = 3/3$ resonance, the radial current density drops to a minimum; however, it increases again at larger radii. A slight axial blowup was also noticeable in this region[17]). During the acceleration from 8 to 12 in. radius, a slow displacement of the apparent center of motion takes place in this case. For the forty-fourth revolution the apparent center of motion has shifted 0.6 in. to the northeast. This effect is probably due to the acceleration occurring in a high magnetic field at the north gap and in a low magnetic field at the south gap. ν_r is approximately 1.01, which leads to a clockwise precession of the orbit centers.

At larger radii the beam centering could be measured by shadow measurements with all three probes. The sharpness and shape of the current cutoff observed in these shadow experiments give information about the distribution of the radial amplitude in the beam. The relative probe positions at the cutoff allow us to evaluate the center displacement. We noticed that good beam quality near the cyclotron center did not necessarily lead to high radial beam quality at larger radii. Quality of the beam was found to be largely dependent on the dee voltage.

Figure 14a and b shows results of shadow measurements at 22 in. radius for two ion-source locations, corresponding to 36- and 50-kV theoretical extraction voltage; the measurements were made at a dee voltage of 36 kV and 45 kV (meter reading). For the lower voltage the coherent radial amplitude,

i. e., center displacement, is approximately 0.3 and 0.5 in. whereas the radial amplitude remains $\approx \pm$ 1/8 in. for both ion-source locations. The higher dee voltage seems to act both times like a first harmonic on the order of 10 G in both bases, displacing the beam center by $\approx$ 1.5 in. and increasing the radial amplitude to $\approx \pm$ 0.5 in.

Figure 14b shows the effect on the radial beam quality at 27 in. radius of a change in the rotation of the source. The radial betatron amplitude can be increased from $\approx \pm$ 1/8 in. at γ = 11 deg to $\approx \pm$ 0.9 in. at γ = 20 deg. The position of the puller remained the same for both measurements.

The effect of a change in the ion-source azimuth θ_s (fig. 9) is indicated in fig. 15. Two extreme positions were investigated. In Case A the ion-source slit was set close to the gap middle line, corresponding to a θ_s of - 5 deg. In Case B the source was moved farther away from the dee, corresponding to a θ_s of - 30 deg. The source-to-puller distance was kept the same in both cases—equivalent to a transit phase angle of $\approx$ 30 deg.

In fig. 15a the total beam currents are given as a function of the radius. Figure 15b shows the currents that were picked up in an axial interval between 1/4 and 3/4 in. above and below the median plane. Figure 15c shows the relative current on the upper and lower electrodes as functions of the radius. The total beam drops rapidly with increasing radius in both Case A and Case B. However, the axial focusing appears to be much better at an ion-source azimuth of θ_s = - 30 deg than in the case of θ_s = -5deg—as is indicated in fig. 15b and c. At a radius of 10 in. the relative amount of beam measured on the pickup electrodes above and below the median plane is larger by a factor of two when the source comes closer to the gap middle line. This result confirms that an appreciable phase lag during the first few revolutions contributes effectively to the overall axial focusing of the beam.

The fast drop of the total current in Case A and Case B in fig. 15a is partly related to phase loss. In the case of $\theta_s = -5$ deg we also observed that a relatively large fraction of the total beam--on the order of 20% --was spilling out radially along the hills, starting from about 5 to 6 in. radius.

For normal starting conditions with $\theta_s = -25$ deg the beam current picked up by the upper and lower electrodes is on the order of 10% and ceases completely after 15 to 20 in. radius. In this case the total beam current stays practically constant from 15 to 38 in. radius. The radially spilling beam was, in the case of α particles at 11.7 kG, practically not noticeable, and certainly smaller than 1%.

Finally, an experiment should be mentioned in which the ion source had been tilted accidentally by about 2 to 3 deg with respect to the vertical axis. In this case the beam consisted of two components, one with a large coherent axial amplitude of ≈ 0.5 in. Photographs were taken of the beam spot on a quartz plate which could be moved radially. Figure 16 shows a time-exposure photograph taken while the quartz probe moved from 23.4 to 4.1 in. radius. It stopped for a few seconds at 18.8, 14.4, and 10.2 in. Separate beam revolutions can be noticed between 4 and 10 in. radius. The modulation of the axial beam oscillation frequency at larger radii can be explained by visually comparing interference of two beam spots having slightly different oscillation frequencies. This is the case when the two beam components have a different phase relationship in the cyclotron. These results show clearly that, for good beam quality, the vertical alignment of the components in the machine center is also of great importance.

We believe that the experimental results mentioned here and observed on other occasions[17]) indicate that our assumptions for the layout studies of the cyclotron center region are justified, at least for smaller beam intensities. With the geometry and parameters present, α beams on the order of 50 to 100μA have been obtainable.

Acknowledgments

The authors wish to express their gratitude to Dr. E. L. Kelly, Mr. W. B. Jones, and the staff of the 88-inch cyclotron for encouragement and guidance in preparing and performing the experiments. We are much obliged to K. W. Ehlers and P. G. Watson for very helpful discussions during the design studies of the center region.

REFERENCES

[1]) F. T. Howard, R. S. Livingston, A. H. Snell and T. A. Welton, Proposal for a Southern Regional Accelerator, ORNL Report CF 57-4-30, April 1957 (unpublished).

[2]) M. M. Gordon, in Sector-Focused Cyclotrons, Proceedings of an Informal Conference, Sea Island, Georgia, Feb. 1959, Nuclear Science Series Report No. 26 (National Academy of Sciences-National Research Council, Washington, D.C., 1959), p. 234.

[3]) H. G. Blosser, in Sector-Focused Cyclotrons, p. 241 (see ref. 2).

[4]) A. A. Garren, Electrostatic-Deflector Calculations for the Berkeley 88-Inch Cyclotron, Lawrence Radiation Laboratory Report UCRL-10067, May 1962, Nucl. Instr. and Method (to be published).

[5]) B. L. Cohen, Rev. Sci. Instr. 24 (1953) 589.

[6]) F. Tintă, N. Martalogu, R. Dumitrescu and T. Magda, Nucl. Instr. and Meth. 12 (1961) 138.

[7]) M. Konrad, The Cyclotron Beam Waveform (Dissertation), University of Birmingham, July 1955.

[8]) M. Reiser, Nucl. Instr. and Meth. 13 (1961) 55.

[9]) C. W. Park and J. JJ Barale, Analog Field Computer: Description and Use, Lawrence Radiation Laboratory Report UCRL-8893, March 1960 (unpublished).

[10]) H. A. Willax, Preliminary Studies on Beam Programming in a Cyclotron Lawrence Radiation Laboratory Report UCRL-9416, Sept. 1960 (unpublished).

[11]) W. I. B. Smith, Nucl. Instr. and Meth. 9 (1960) 49.

[12]) P. G. Watson, Development of the Magnetic Cone for the Center of the Berkeley 88-Inch Cyclotron, Lawrence Radiation Laboratory Report UCRL-10072, May 1962, Nucl. Instr. and Meth. (to be published).

[13]) Baron Manfred von Ardenne, Tabellen der Electronenphysik, Ionenphysik, und Übermikroskopie (Deutscher Verlag der Wissenschaften, Berlin, 1956).

[14]) J. E. Stover, Rapid Traversal of 3/3 Radial Resonance Near the Center of a Sector Focused Cyclotron, Michigan State University Report MSUCP-3, Aug. 1960 (unpublished).

[15]) K. W. Ehlers, Design and Development of the Ion Source for the Berkeley 88-Inch Cyclotron, Lawrence Radiation Laboratory Report UCRL-10080, Feb. 1962, Nucl. Instr. and Meth. (to be published).

[16]) J. M. Haughian and R. J. Burleigh, The Ion-Source Mechanism for the Berkeley 88-Inch Cyclotron, Lawrence Radiation Laboratory Report UCRL-10068, March 1962, Nucl. Instr. and Meth. (to be published).

[17]) E. L. Kelly, General Description and Operating Characteristics of the Berkeley 88-Inch Cyclotron, Lawrence Radiation Laboratory Report UCRL-10081, April 1962, Nucl. Instr. and Meth. (to be published).

FIGURE CAPTIONS

Fig. 1. Equipotential lines in a vertical cross section.

(a) With a single dee.

(b) With a dee and a dummy dee.

(The numbers near the equipotential lines indicate percent of dee voltage.)

Fig. 2. Potential and electric field across the acceleration gap, with and without a dummy dee.

(a) Electric potential in the median plane.

(b) Horizontal component of the electric field in the median plane; 70-kV dee voltage.

(c) Vertical component of the electric field 0.25 in. above and below the median plane; 70 kV dee voltage.

Fig. 3. Equipotential lines in the median plane near the source and puller, as measured in the electrolytic tank.

(a) Sketch of the puller.

(b) Single-dee geometry.

(c) Dee and dummy-dee geometry.

(The numbers near the equipotential lines indicate percent of dee voltage.)

Fig. 4. Equipotential lines in the median plane, as measured in the electrolytic tank for a single dee and a puller post. (The numbers near the equipotential lines indicate percent of dee voltage.)

Fig. 5. Geometric orbit study for (a) a single dee and (b) a dee and dummy-dee configuration

Procedure for orbit plotting:

Step-by-step momentum gain each 30 deg.

Basic parameters:

Magnetic field H = const = 16.5 kG

Mass to charge ratio $\frac{A}{q}$ = 2 (deuterons)

Frequency $\omega = \omega_0$ = 12.7 Mc/sec

Dee voltage U_0 = 70 kV

(The apparent centers of motion after the third revolution are marked. The numbers at both ends of the equipotential lines indicate percent of dee voltage.)

Fig. 6. Transit-time factor for idealized step acceleration at the center of the gap, as derived from the geometric orbit study.

Fig. 7. Geometric orbit study for particles with an initial divergence corresponding to ± 1/8 in. radial amplitude for a single-dee configuration. Basic parameters and procedures as in Fig. 5. (The numbers at both ends of the equipotential lines indicate percent of dee voltage.)

Fig. 8. Electric and magnetic axial focusing terms for a single-dee configuration. Values for $\nu_z{}^2{}_{el}$ are derived from numerical integration of the beam trajectories through the first three revolutions. The curve of $\nu_z{}^2{}_{mag}$ corresponds to the field shape used for α particles at 11.67 kG.

Fig. 9. Schematic of the ion starting conditions.

Fig. 10a, b, c, d. Relative initial energy gain and initial coordinates of the center of motion as functions of the starting phase and the phase at the puller slit.

e. Areas A and B are indicative of the intensity in a beam pulse of an initial center spread of less than 1/16 in.

f. Relationship of starting trajectories for particles with maximum energy gain (R_m) and particles starting in phase (R_0).

Case A: Transit-time angle τ_0 = 20 deg [for the particles starting in phase (ϕ_0 = 0 deg)].

Case B: Transit-time angle τ_0 = 40 deg (for the particles starting in phase).

Parameters: α particles,

B = 11.67 kG,

U_0 = 36 kV.

Fig. 11. Schematic drawing of the center geometry in the cyclotron. Shown are a proposal position for the defining slit, together with possible position changes of one tantalum bar with respect to the other.

Fig. 12. The puller face as seen from the ion source. (The vertical free space within the puller is 1/2 in.)

Fig. 13. Perspective view of the center region out to 12 in. radius, with first four computed revolutions and reliefs of the α-beam current distribution as measured with the dee area probe (left) and deflector area probe (right). The predicted (0) and apparent (x) centers of motion for the second and forty-fourth revolutions are shown.

Parameters:

$B_{0\,is}$ = 11.67 kG,

f = 8.98 Mc/sec,

U_0 ≈ 36 kV.

Fig. 14. Radial shadow measurements at 22- and 27-in. probe radius for different starting conditions.

(a) Ion-source position for U_0 = 36 kV; dee voltage 36 kV and 45 kV (meter values).

(b) Ion-source position for U_0 = 50 kV; dee voltage 36 kV and 45 kV (meter values).

(c) Ion-source position for U_0 = 36 kV; dee voltage 36 kV (meter values). Source rotation angle γ = 11 and 20 deg.

Fig. 15. Total and axial beam distribution for two azimuthal values of θ_s that were deliberately set so as to deviate from the theoretical.

Case A: Ion source and puller moved azimuthally towards center of gap, θ_s = - 5 deg. Case B: Ion source moved azimuthally to where θ_s = - 30 deg.

(a) Total current vs radius.

(b) Current on upper and lower pickup electrode (1/4 in. $\leq |z| \leq$ 3/4 in.).

(c) Relative current on upper and lower electrodes.

Fig. 16. Beam pattern shown by a quartz probe 1/16 by 15/8 by 15/8 in., moved from 23.4 to 4.1 in. radius and stopped at 18.8, 14.4, and 10.2 in. radius.

(Beam current about 5 μA; ion source tilted from vertical axis by approx 3 deg.)

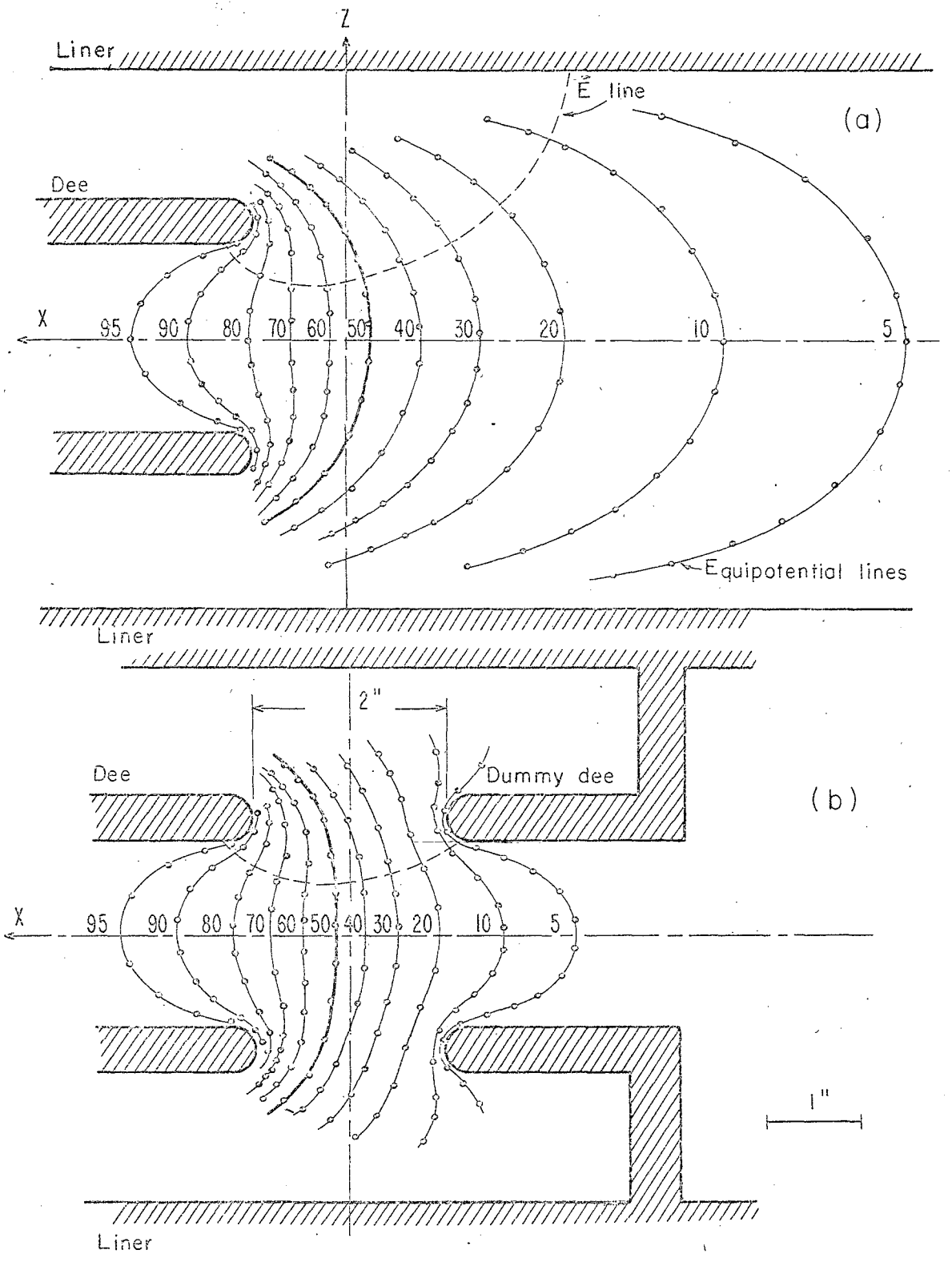

MU-26313

UCRL-10071

Fig. 1

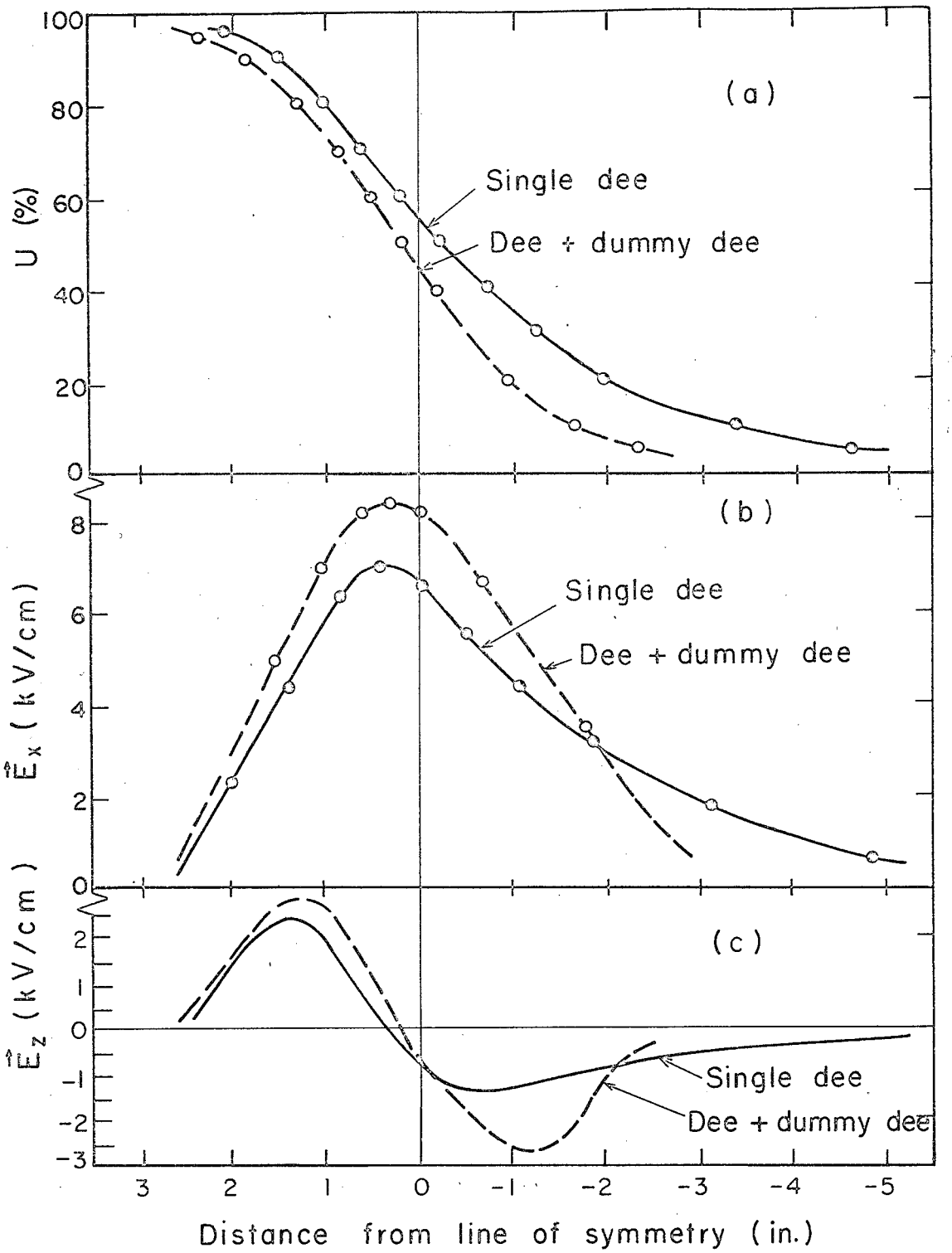

MU-26322

UCRL-10071

Fig. 2

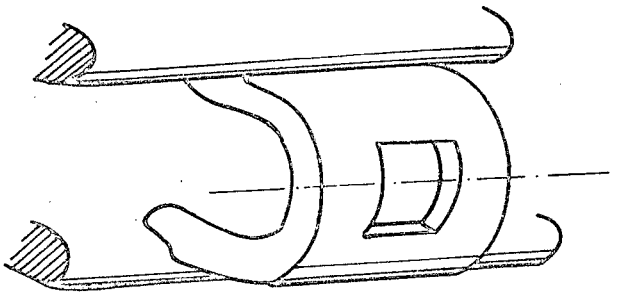

(a)

(b)

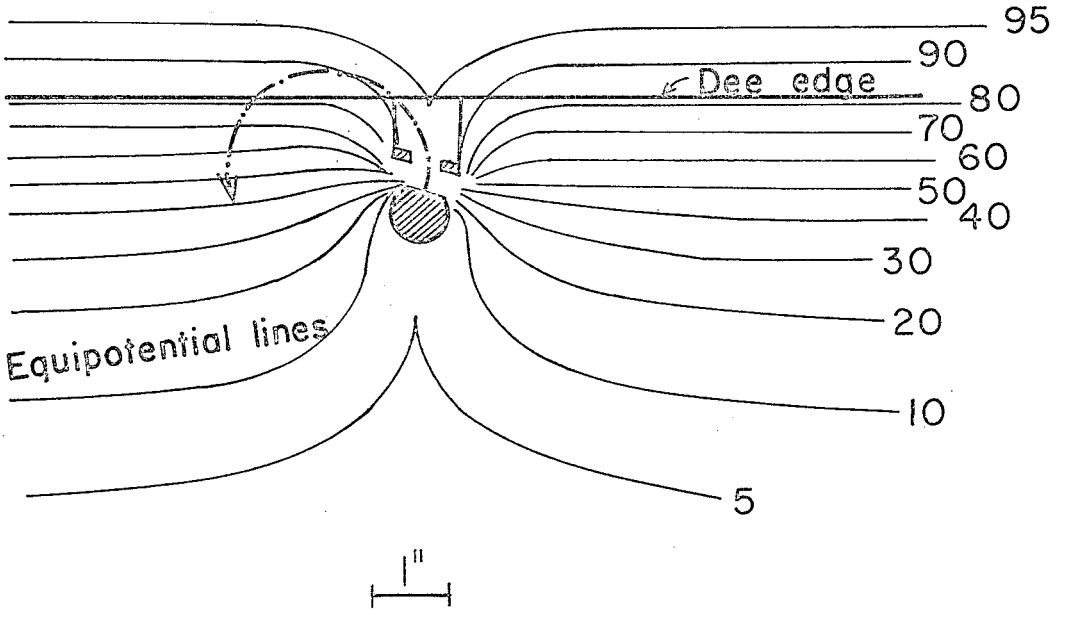

(c)

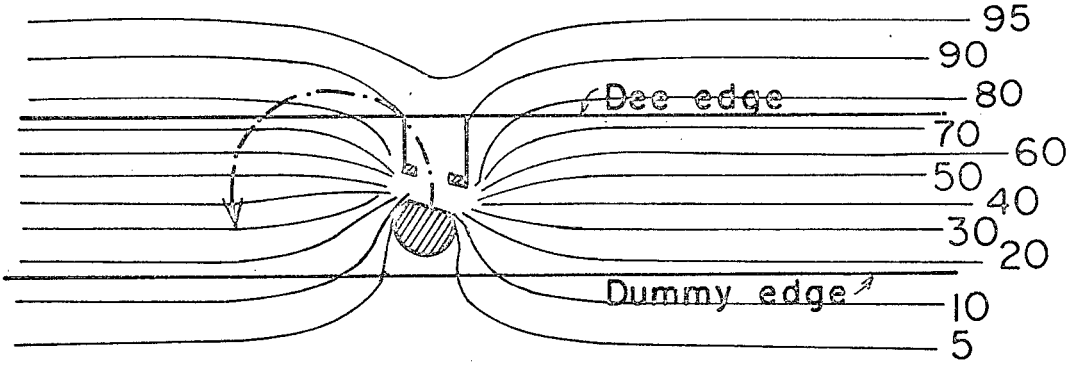

MU-26311
UCRL-10071
Fig. 3

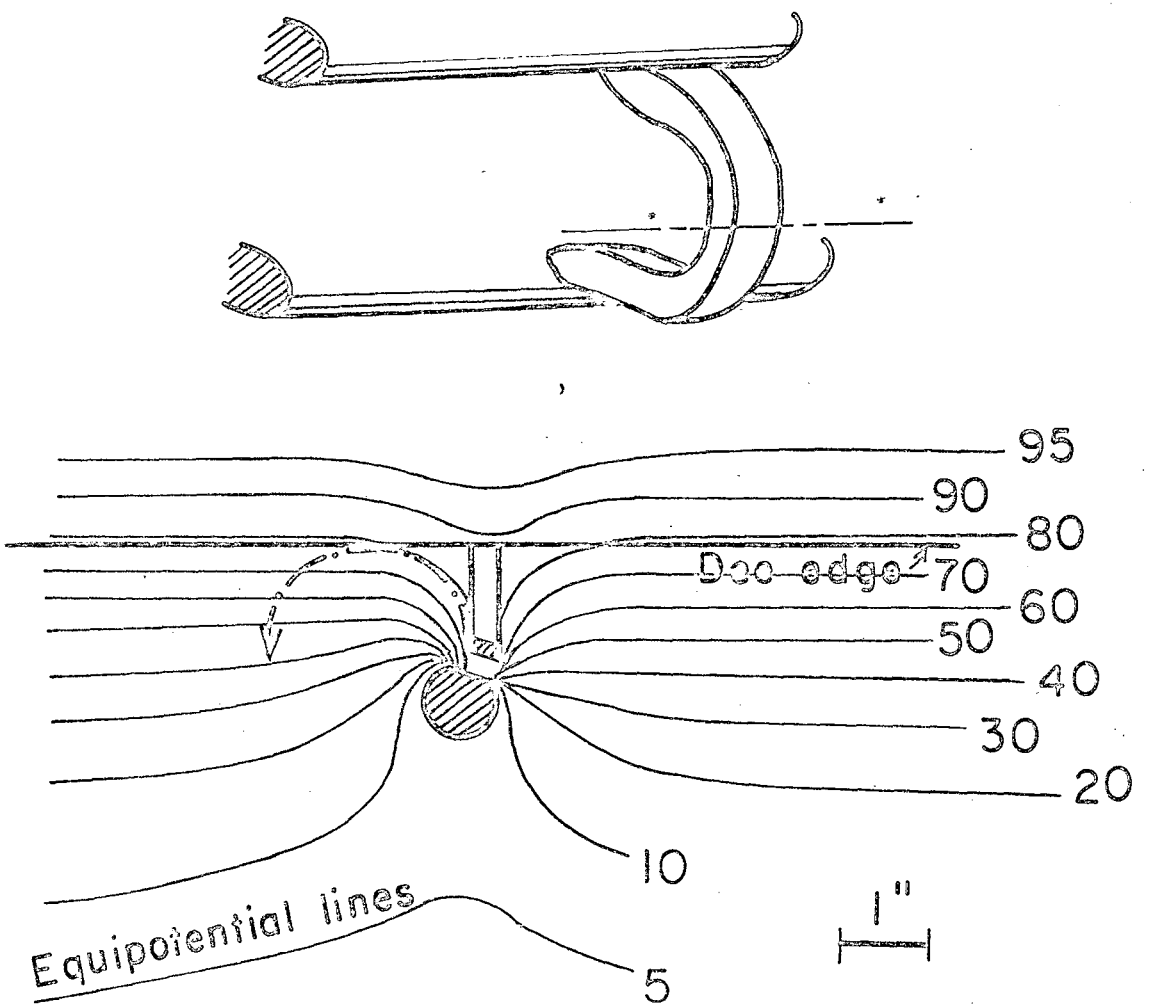

MU-26321
UCRL-10071
Fig. 4

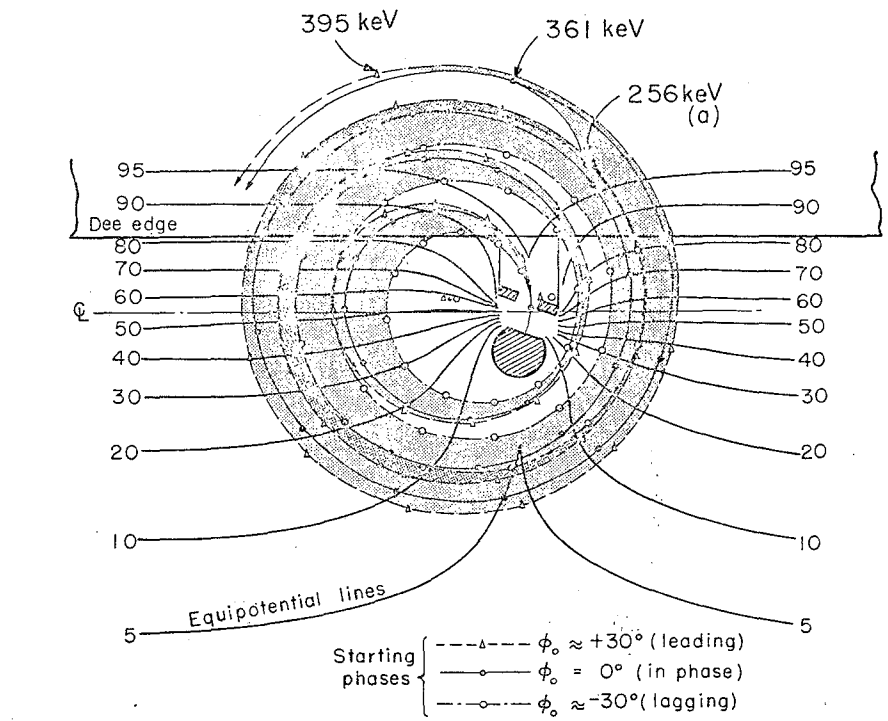

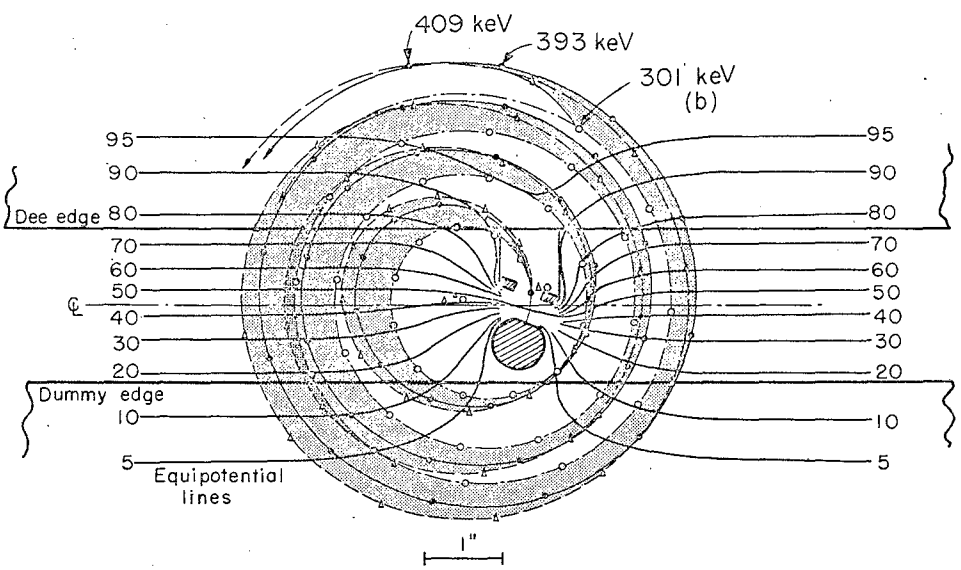

MUB-985

UCRL-10071
Fig. 5

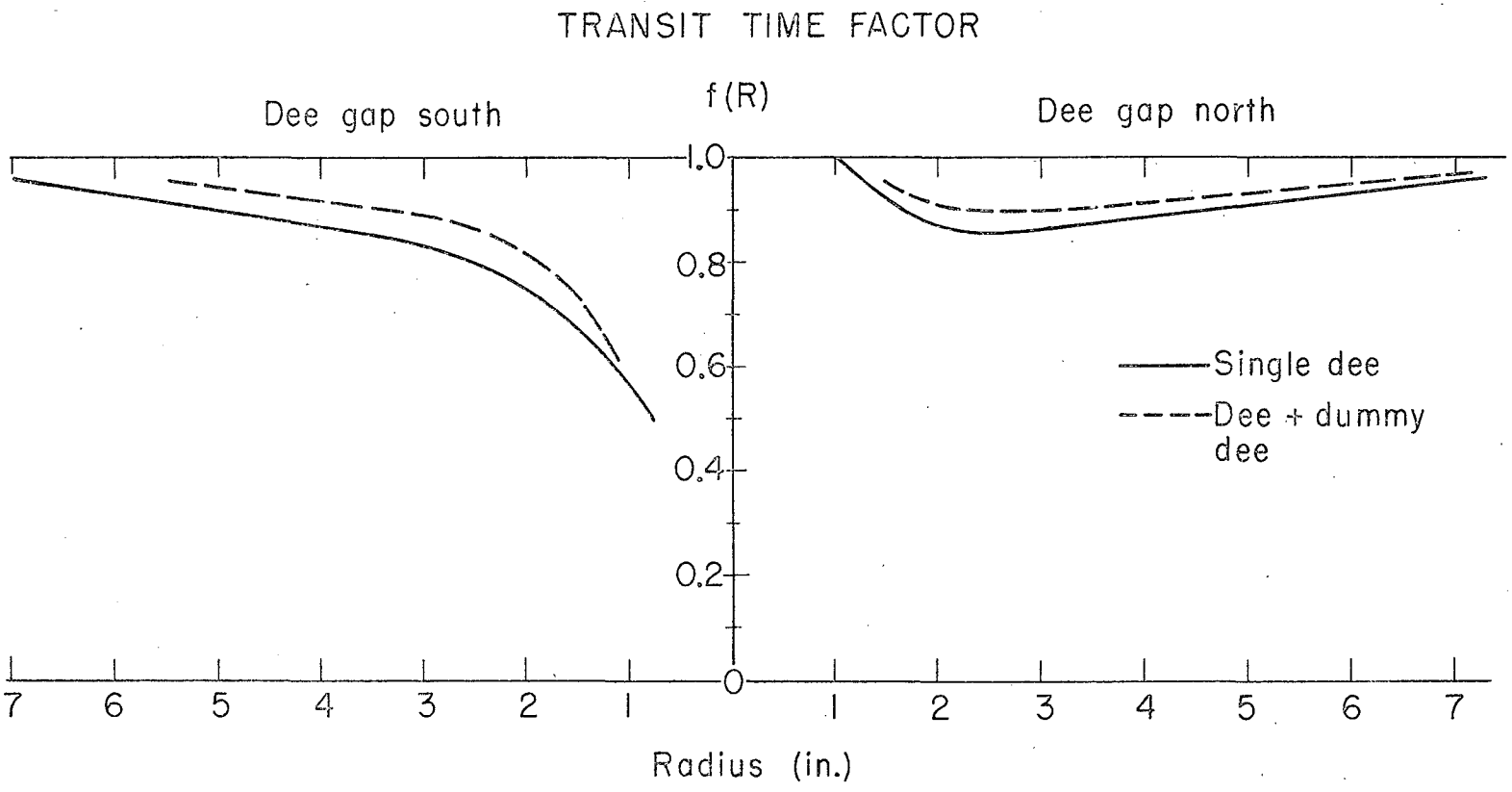

MU-26312

UCRL-10071

Fig. 6

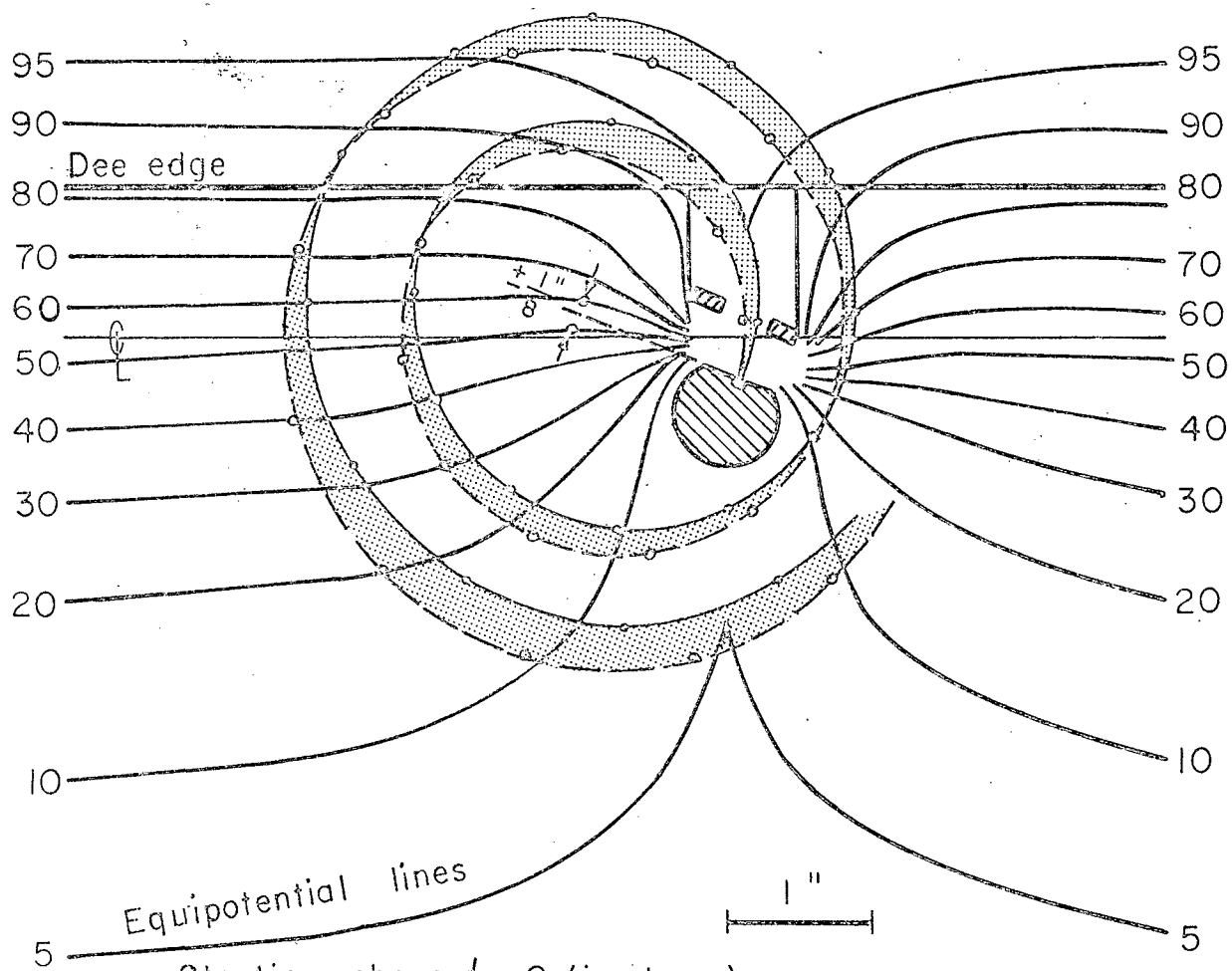

Starting phase: $\phi_0 = 0$ (in phase)

Radial amplitude:

——o—— = + 1/8"

— — —o— — — = — 1/8"

MU-26315

UCRL-10071

Fig. 7

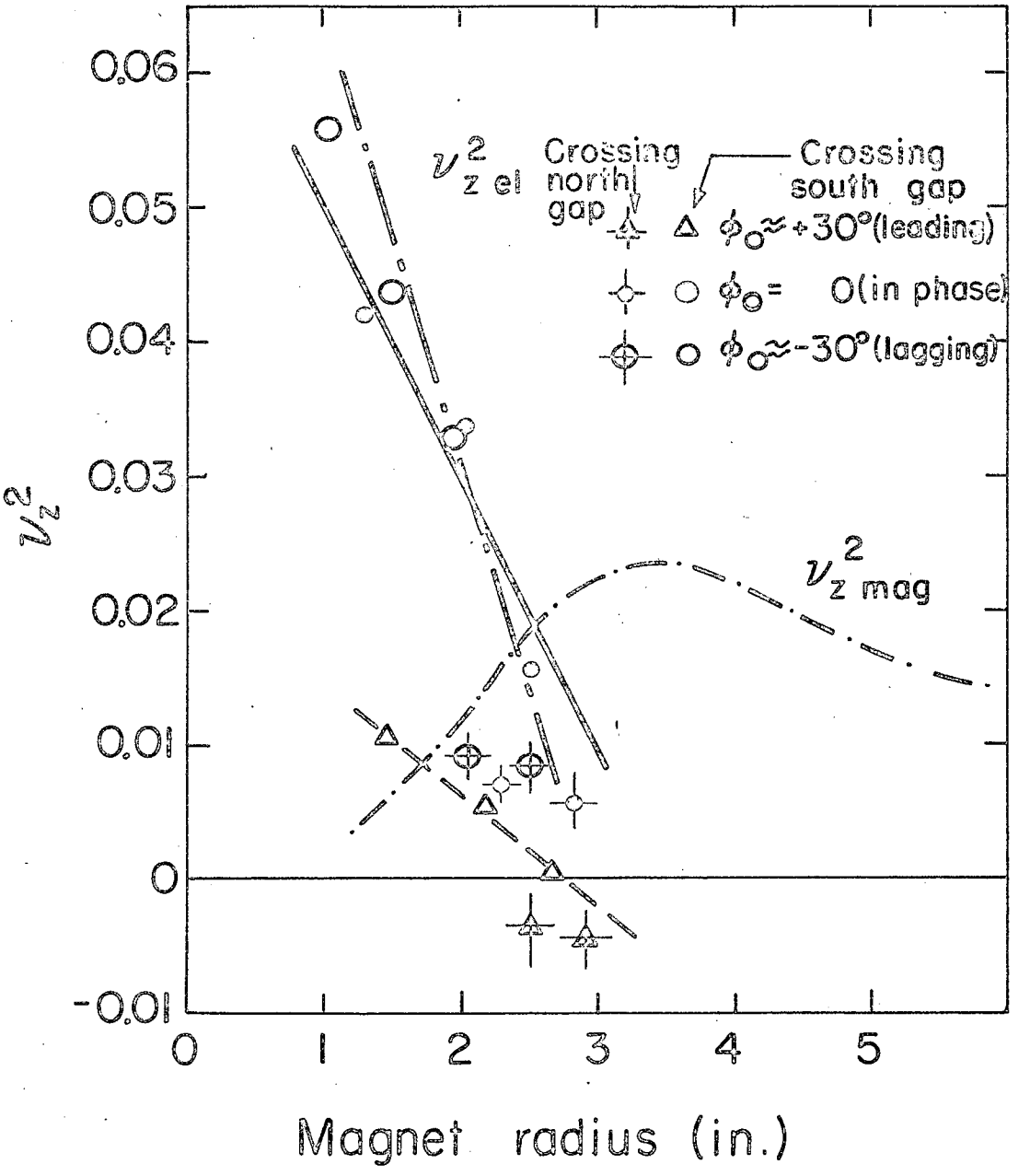

MU-26349
UCRL-10071
Fig. 8

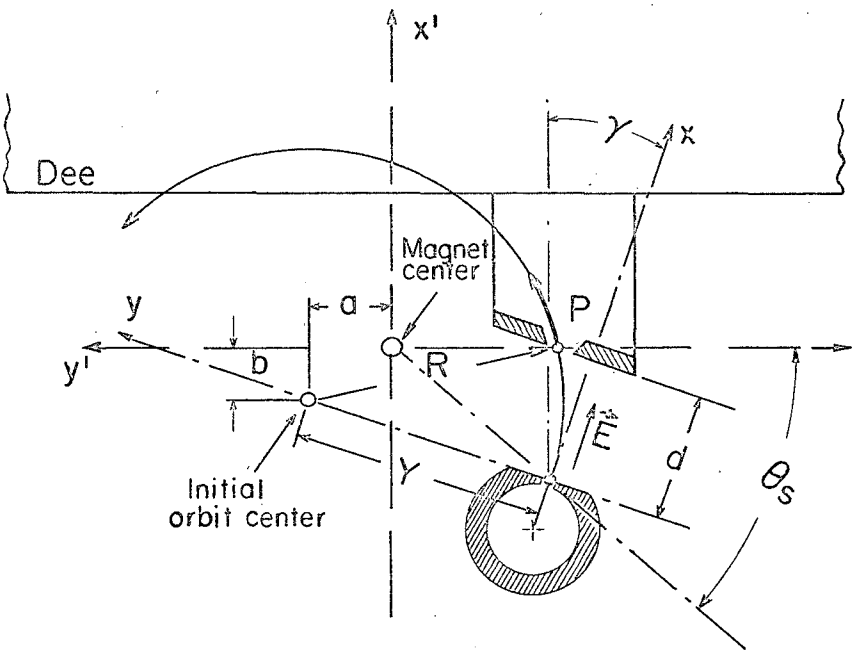

MUB-1014

UCRL-10071

Fig. 9

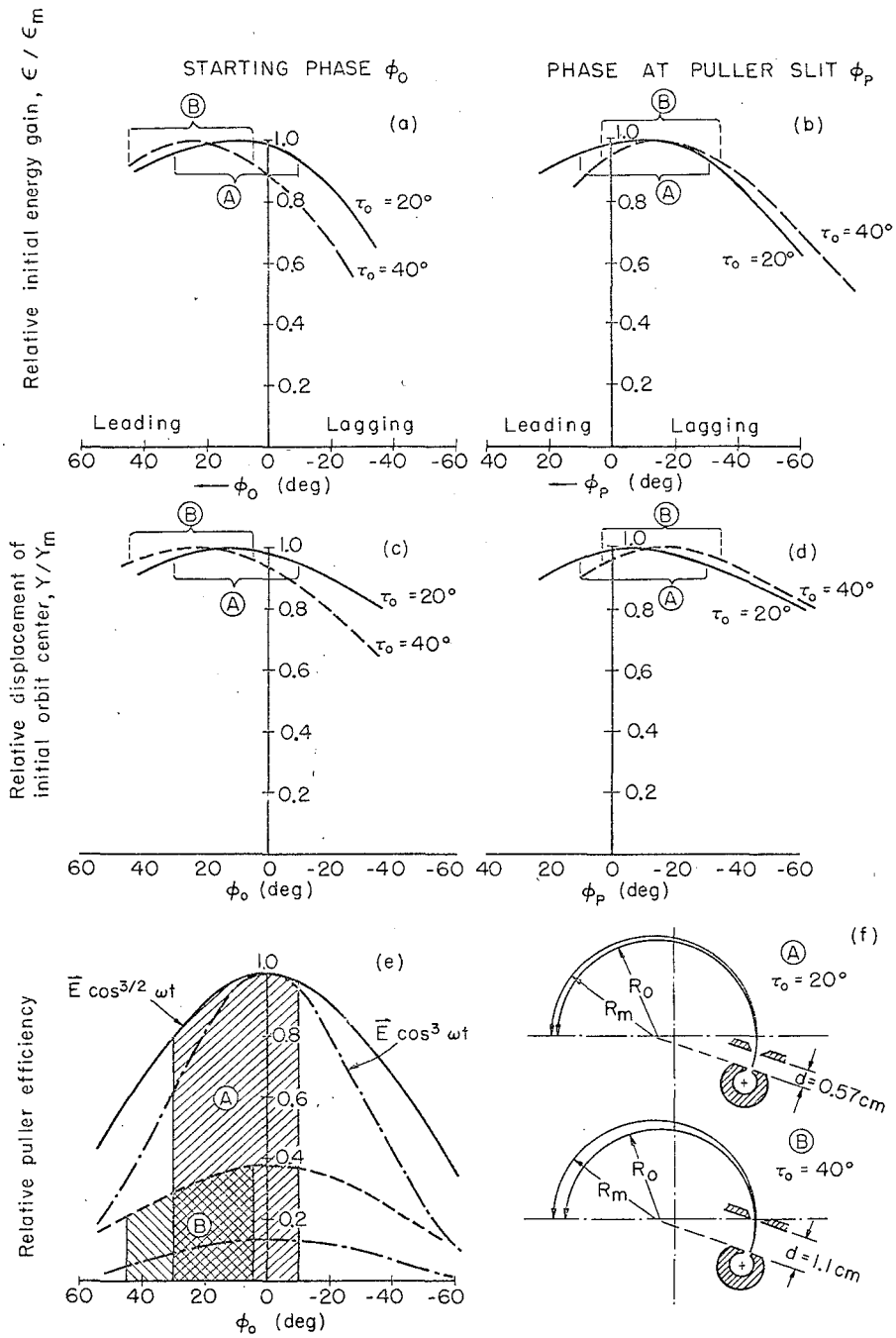

MUB-1012

UCRL-10071
Fig. 10

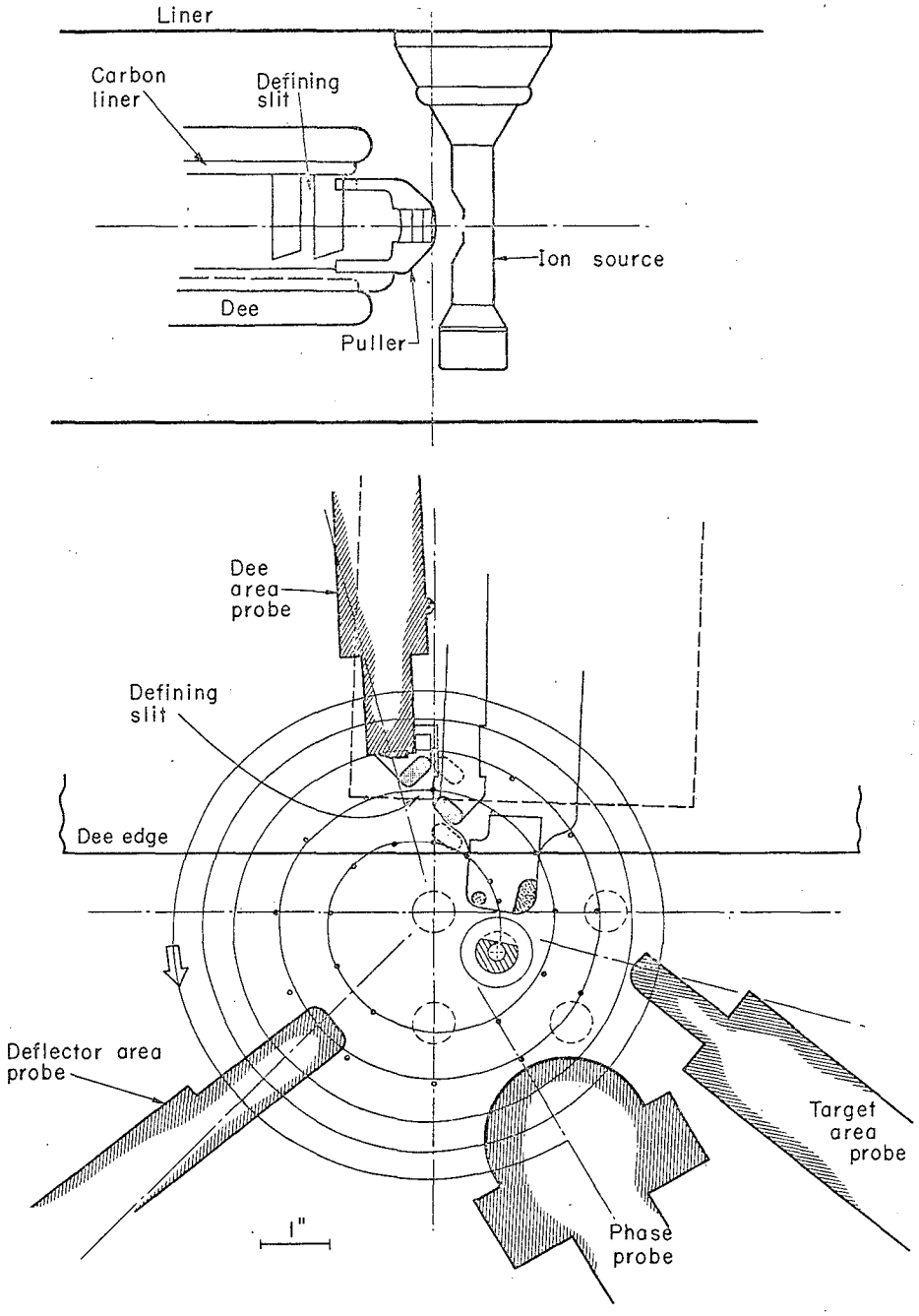

MUB-993

UCRL-10071
Fig. 11

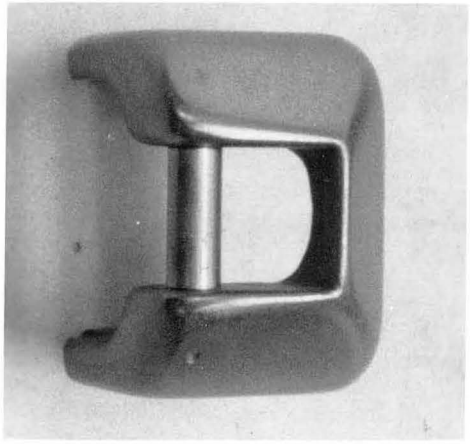

12

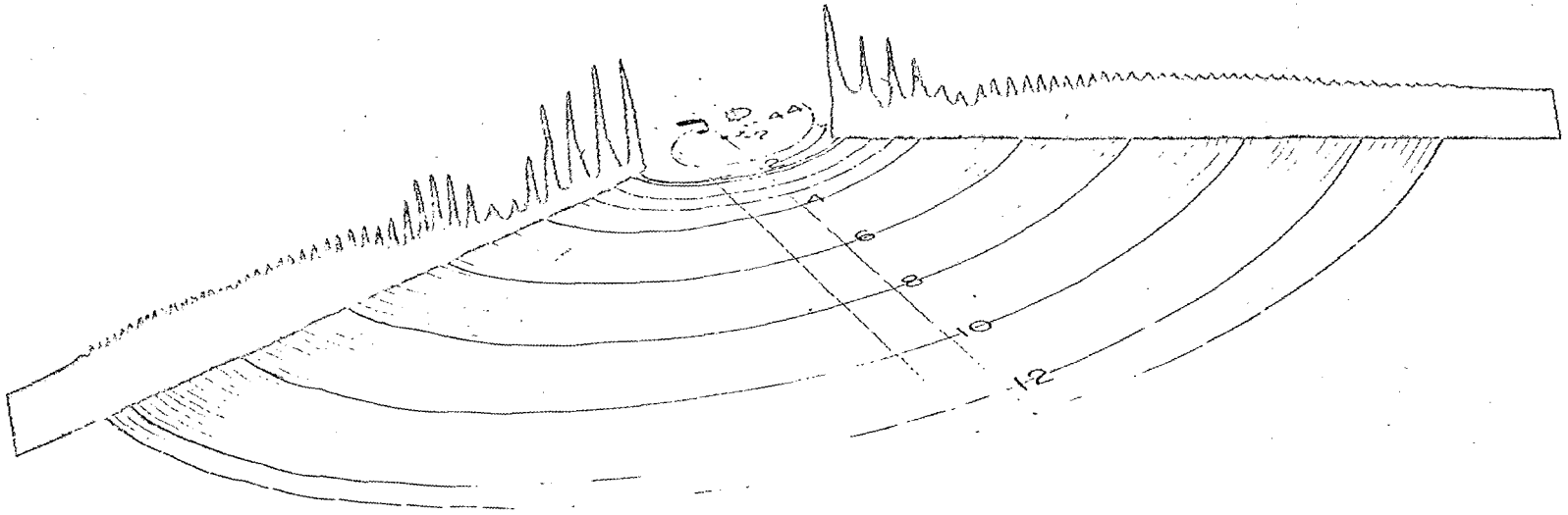

MUB-1002
UCRL-10071
Fig. 13

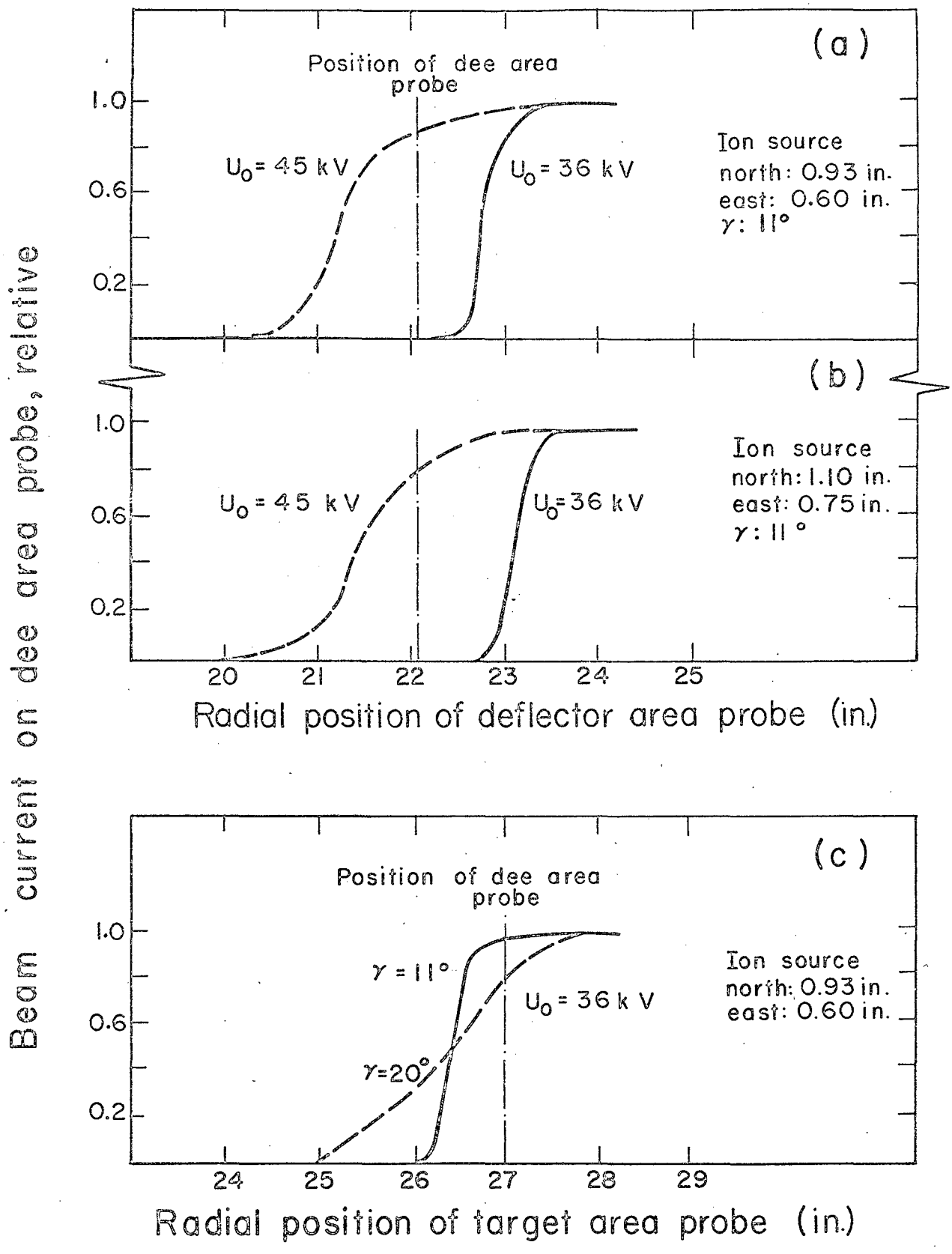

MU-26533

UCRL-10071

Fig. 14

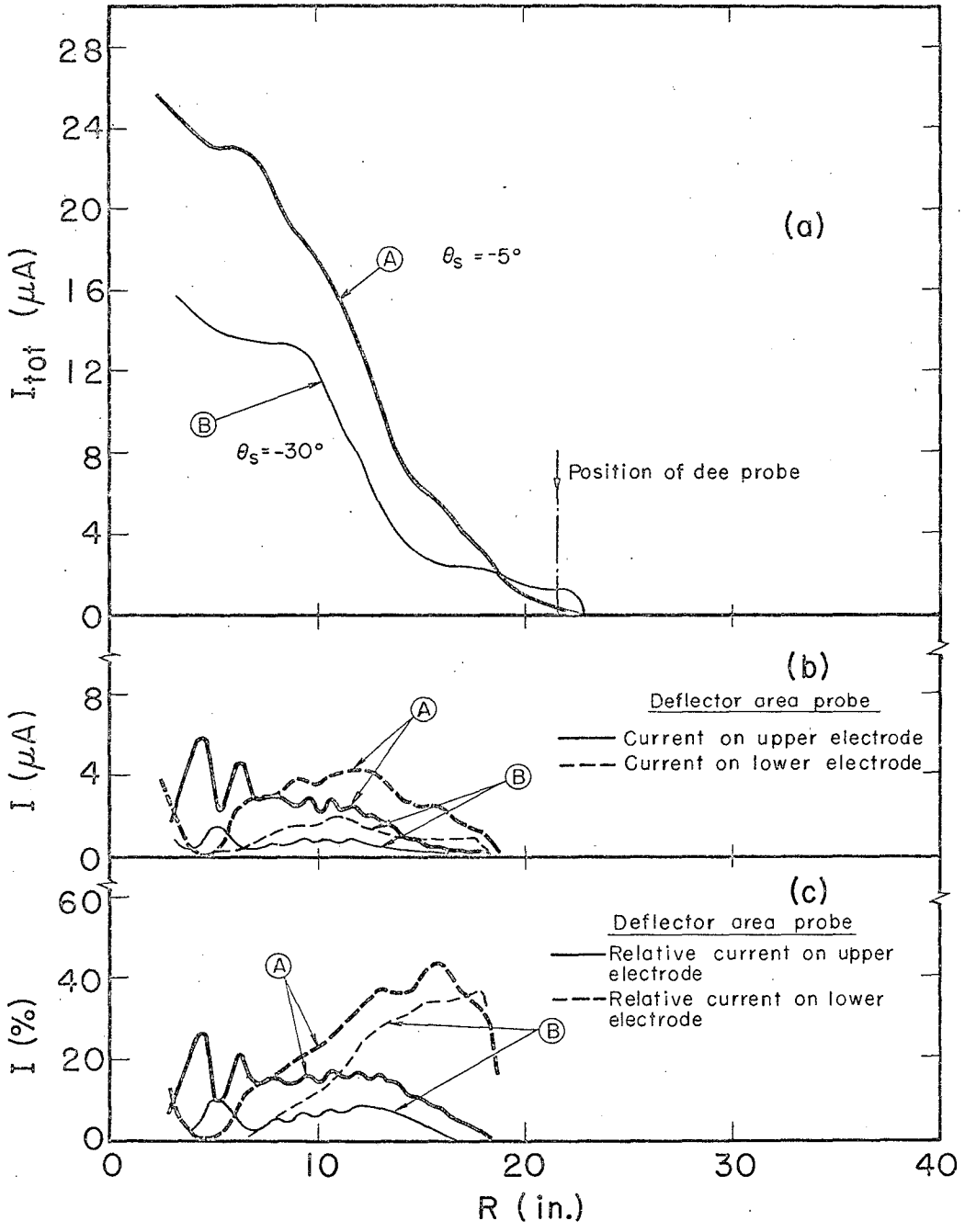

MUB-1011

UCRL-10071

Fig. 15

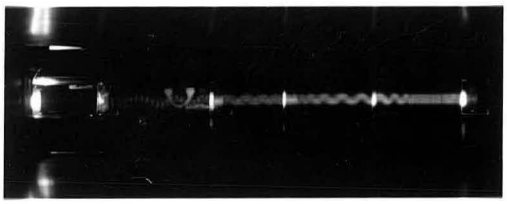

16